Pergamon

Bioorganic & Medicinal Chemistry, Vol. 3, No. 8, pp. 1009–1017, 1995

0968-0896/95 $9.50 + .00

0968-0896(95)00096-8

Crystallographic Structure of a Peptidyl Keto Acid Inhibitor and Human α-Thrombin

Kjell Håkansson,[a] A. Tulinsky,*[a] Matthew M. Abelman,[b] Todd A. Miller,[b] George P. Vlasuk,[b] Peter W. Bergum,[b] Marguerita S. L. Lim-Wilby[b] and Terence K. Brunck*[b]

[a]*Department of Chemistry, Michigan State University, East Lansing, MI 48824-1322, U.S.A.*
[b]*Corvas International, Inc., 3030 Science Park Road, San Diego, CA 92121-1102, U.S.A.*

Abstract—The low molecular weight α-keto amide inhibitor CVS-1347, benzyl-SO_2-Met(O_2)-Pro-Arg(CO)((CONH)CH_2)-phenyl, is a slow, tight binding inhibitor of α-thrombin amidolytic activity having a K_i = 1.28 × 10^{-10} M. A complex between human α-thrombin and a hydrolysis product of CVS-1347 has been determined and refined using crystallography. The crystals belong to monoclinic space group C2 with cell dimensions of a = 71.08, b = 72.05 and c = 72.98 Å and β = 100.8°. The structure was solved using isomorphous replacement methods and refined with resolution limits of (8.00–1.76) Å to an R-value of 0.162. The Pro–Arg core of the inhibitor binds in the S2 and S1 subsites respectively, as is usually observed for Pro-Arg thrombin inhibitors. The Met(O_2) side chain does not make any close contacts with the enzyme but influences the conformation of Glu192; the N-terminal benzylsulfonyl group makes an aromatic–aromatic contact with Trp215 in the hydrophobic part of the active site. The α-keto carboxylic acid of the proteolyzed inhibitor binds with the carboxylate group in the oxyanion hole, demonstrating that this region can accommodate an anion in a protease–peptide complex. The α-keto carbonyl group interacts closely with the two most important residues in the active site: the carbon atom is within a covalent bond distance of the active site Ser195 Oγ and the carbonyl oxygen is hydrogen bonded to His57. These residues thus act as a Lewis acid and base in catalysis with respect to the substrate carbonyl carbon and peptide nitrogen atoms of the scissile bond of substrate.

Introduction

Thrombin (EC 3.4.21.5) is the terminal serine protease in the blood coagulation cascade that catalyzes the proteolytic cleavage of fibrinogen, resulting in the polymerization of the fibrin product into an insoluble gel.[1] Thrombin is composed of a 259-residue heavy chain containing the catalytic triad of His57, Asp102, Ser195 and a smaller 36-residue light chain, connected to each other through a single disulfide bridge. The amino acid sequence of the heavy chain of thrombin, like other blood coagulation proteases, displays a high degree of homology (~50%) to other serine proteases of the trypsin family[2,3] and has a similar fold consisting of two six-stranded antiparallel β-barrels.

Since thrombin is autolytic, the crystallographic structure of the human enzyme was solved initially using an inhibitor complex.[4] In addition to showing the general, trypsin-like fold, this and other thrombin-liganded structures have also yielded important information about substrate recognition and the macromolecular operative mode of the enzyme.

The natural peptide inhibitor hirudin originally isolated from the leech[5,6] binds with its N-terminus in the active site of thrombin and with the remainder of the molecule stretching to the fibrinogen binding exosite.[7] The synthetic C-terminal analog of hirudin, hirugen, which comprises only 12 residues, occupies the fibrinogen exosite only.[8] These binding characteristics enable the formation of ternary complexes of thrombin, hirugen and active site inhibitors that crystallize isomorphously.[8,9]

Direct inhibitors of thrombin catalytic activity have been demonstrated to have important pharmacological effects in the attenuation of the thrombotic process both in experimental models of thrombosis as well as clinically.[10] A number of approaches have been explored in the development of direct thrombin inhibitors, resulting in a wide variety of chemical structures that target not only the primary catalytic site of the enzyme, but also other recognition sites outside the active site.[11,12] However, in the design of thrombin inhibitors that are orally active, it is imperative that the molecular weight of the molecule be small (< 500 g mol^{-1}) and that there are a limited number of amide bonds that may be susceptible to proteolytic degradation. Therefore, virtually all of the current attention in the design and synthesis of small molecule thrombin inhibitors has focused on those types of compounds, which bind with high affinity to the catalytic site of the enzyme. Many of these molecules contain a chemical group that serves as a transition state mimetic, allowing stable inhibition of catalytic activity through the formation of a tetrahedral intermediate with the enzyme upon binding. Of the various forms of transition state analogs, the α-keto amide group has been shown to be extremely effective. Previous studies of a naturally occurring inhibitor, cyclotheonamide A, that contains an arginine-α-keto amide residue, have shown the

direct coordination of the α-carbonyl with the active site serine of thrombin and trypsin.[13-15] α-Keto amide thrombin inhibitors are unique among the class of transition-state inhibitors in that they permit the design and synthesis of new small molecule inhibitors that can probe the S′ subsites and fibrinogen exosite binding regions of thrombin.

We now report the first structure of a keto acid thrombin inhibitor, benzyl-SO_2-Met(O_2)-Pro-Arg(CO)-OH, derived from a potent α-keto amide inhibitor CVS-1347 (Fig. 1) in its ternary complex with thrombin and hirugen.

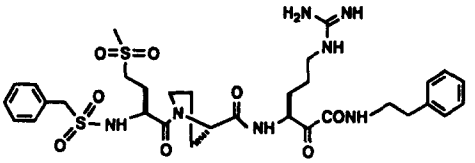

Figure 1. Molecular structure of CVS-1347.

Results

The kinetics of α-thrombin inhibition by CVS-1347 were investigated by monitoring the inhibition of amidolytic activity using a peptidyl chromogenic substrate. Preliminary experiments in which CVS-1347 was preincubated with α-thrombin for various times prior to the addition of the chromogenic substrate suggested that a steady state level of inhibition was achieved slowly over a period of 30–40 minutes. These results were confirmed and extended as shown in Figure 2A in which the steady-state level of inhibition was slowly established following the addition of α-thrombin to a fixed concentration of chromogenic substrate in the presence of increasing inhibitor. The analysis of these progress curves using the relationships developed by Cha[16] and Williams and Morrison[17] for competitive, slow-binding inhibitors indicated that the mechanism governing the interaction of CVS-1347 with α-thrombin was most consistent with the formation of a single EI complex as demonstrated by the linear relationship between the apparent first-order rate constant (k_{obs}) and inhibitor concentration [I] as shown in Figure 2B. The rate of association ($k_1 = 1.64 \pm 0.26 \times 10^6$ M^{-1} s^{-1}), rate of dissociation ($k_{-1} = 2.11 \pm 0.09 \times 10^{-4}$ s^{-1}) and equilibrium constant for the dissociation of the EI complex ($K_i = k_{-1}/k_1 = 1.29 \pm 0.06 \times 10^{-10}$ M), were derived from this analysis using equation 2 as described in the Experimental.

In our investigations of low molecular weight inhibitors containing the α-keto amide functional group, we found that some arginine keto amides are somewhat more labile toward hydrolysis than their corresponding amides. However, CVS-1347 was the only keto amide case where hydrolysis occurred during crystallization out of five examples where we have determined structures of these inhibitors with thrombin (unpublished results of the MSU laboratory). No hydrolysis of CVS-1347 was observed during the kinetic assays and, although the keto acid is also an inhibitor of thrombin, CVS-1347 is probably not a prodrug in the strictest sense. The hydrolysis in this case provides an opportunity to study the binding mode of another arginine keto acid, which binds markedly different from that of the *p*-amidinophenylpyurate (APP) in its complex with trypsin.[18]

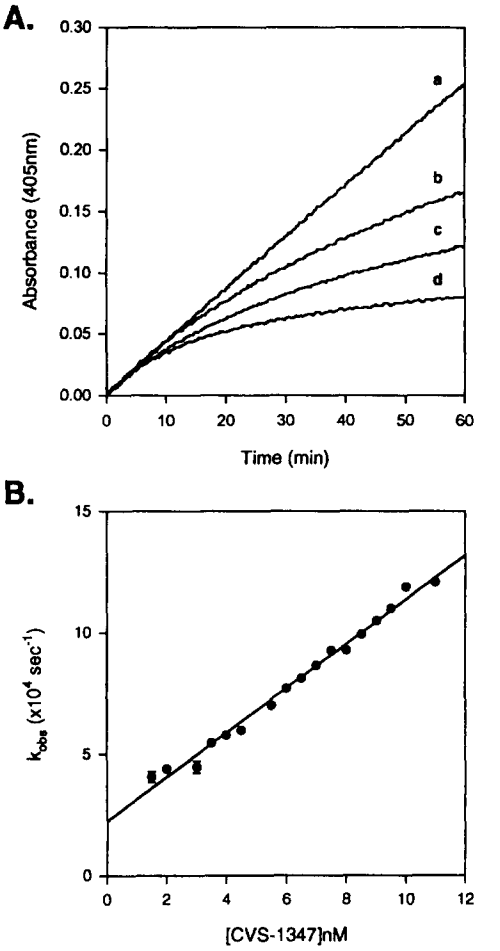

Figure 2. Kinetics of α-thrombin inhibition by CVS-1347. (A) Progress curves illustrating the time-dependent, slow inhibition of α-thrombin amidolytic activity by CVS-1347. Tracings a–d were recorded over 60 min following the addition of α-thrombin to a mixture containing 750 μM chromogenic substrate and CVS-1347 at the final concentrations of (a) 0, (b) 4 nM, (c) 6 nM, and (d) 12 nM as described in the Experimental. (B) Relationship between the apparent first-order rate constant (k_{obs}), and the concentration of CVS-1347. Progress curves similar to those shown in Figure 1A were generated over a concentration range of 0–12 nM CVS-1347 and k_{obs} calculated using equation 1 described in the Experimental. The solid line represents the best fit of the data to equation 2 described in the Experimental ($r = 945$) and was used to calculate k_1 ($1.64 \pm 0.26 \times 10^6$ M^{-1} s^{-1}), k_{-1} ($2.11 \pm 0.09 \times 10^{-4}$ s^{-1}) and K_i ($1.29 \pm 0.061 \times 10^{-10}$ M) at the fixed substrate concentration of 750 μM and the predetermined value of K_m of 45 μM. The data represent the mean of three experiments.

The structures of the thrombin and hirugen components and the nature of their interactions as previously reported[8] are unaffected by the presence of the inhibitor in the active site of thrombin of the ternary complex. The root mean square difference of C_α positions for the heavy chain of thrombin in the two structures is only 0.3 Å.

Some parts of the hirugen (Asn52–Gly54 and side chains of Glu58, Glu61 and Leu64), the termini of the thrombin light chain (Thr1H–Gly1F and Asp14L–Arg15) and the autolysis loop of the thrombin heavy chain (Trp148–Lys149E) could not be defined due to lack of electron density signals. The CVS-1347 inhibitor itself displayed no electron density beyond the C-terminal amide bond (Fig. 3) and a matrix-assisted laser desorption ionization mass spectroscopy (MALDI–MS) measurement of crystalline material confirmed that the phenethylamine group was cleaved from the remainder of the inhibitor at this site. Since CVS-1347 was well characterized by NMR and mass spectroscopy prior to its use in the crystallization experiments, cleavage must have occurred during the crystallization itself.

The proline residue and the arginine side chain of the cleaved inhibitor bind to thrombin in a similar way to the corresponding residues of the prototypical Pro–Arg inhibitor D-Phe-Pro-Arg chloromethyl ketone (PPACK).[4,9] The positions of the two residues are compared with those of PPACK in PPACK–thrombin (Fig. 4), whereas Figure 5 is a schematic representation of the hydrogen bonds involved. The arginine side chain is bound in the S1 subsite with the guanidinium group stacked between the peptide nitrogen atoms of Cys191 and Gly216, with Nη1 and Nη2 additionally forming a doubly hydrogen bonded salt bridge with the carboxylate atoms of Asp189 (2.9 and 2.7 Å, respectively). Moreover, Nη2 is hydrogen bonded to the main carbonyl oxygen of Gly219 (2.9 Å) and Nη1 is hydrogen bonded to a water molecule (3.1 Å), which in turn interacts with Phe227 O (3.1 Å). Another conserved water molecule hydrogen bonds between Nε of the arginine and Gly219 O. The peptide nitrogen of the hydrolyzed derivative is at a longer distance (3.3 Å) from the carbonyl oxygen of Ser214. The proline side chain makes hydrophobic contacts with several residues in the S2 subsite of thrombin and is within 4.0 Å of the His57, Tyr60A, Trp60D, Leu99 and Trp215 side chains, and Ser214 O. The carbonyl oxygen of the proline hydrogen-bonds to a water molecule (2.9 Å). The side chain of the methionine sulfone residue displays a high degree of thermal motion and is not well defined. In its refined

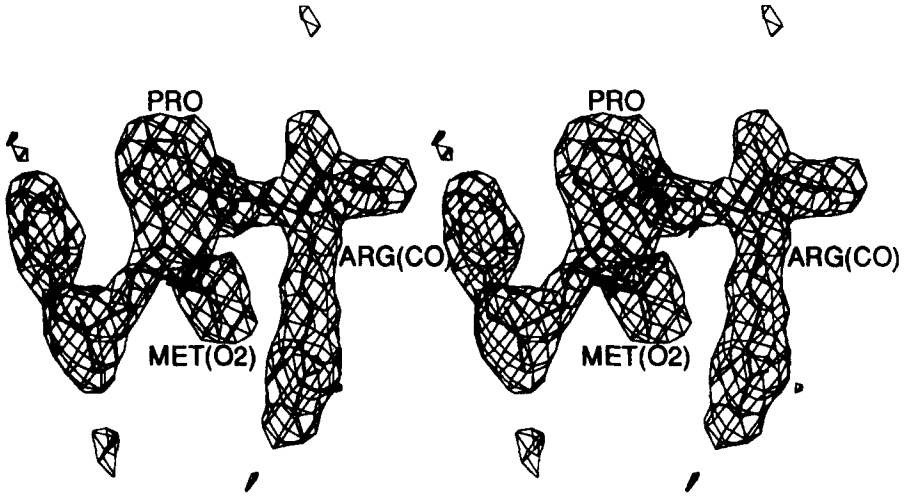

Figure 3. Stereoview of omit map at the inhibitor position drawn at 3σ level. The (| Fo | – | Fc |) map was calculated after refinement with the inhibitor omitted.

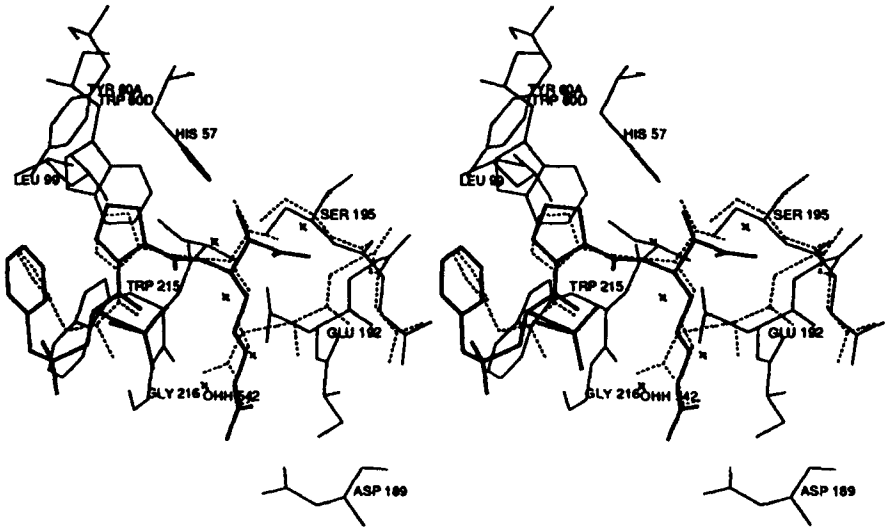

Figure 4. Stereo representation of the binding of the hydrolysis adduct of CVS-1347 in the active site of thrombin. The inhibitor is drawn with a thicker line than the enzyme; PPACK and the Glu192–Ser195 stretch in the monoclinic PPACK–hirugen–thrombin structure[9] is shown with a broken line; covalent bonds from PPACK to His57NE2 and α-keto of CVS-1347 to Ser195OG are not shown.

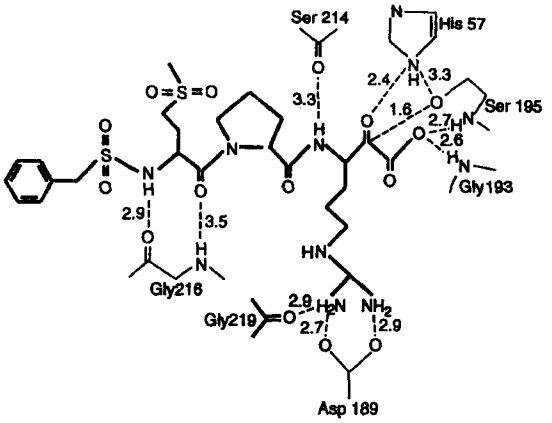

Figure 5. Schematic of hydrogen bond contacts between hydrolyzed inhibitor CVS-1347 and α-thrombin. Distances in Å.

position, it is pointing out to the solvent and makes no contact below 3.7 Å with the enzyme but is hydrogen bonded to two water molecules, one of which is also hydrogen bonded to Gly219N. The electronegative OE2 of the sulfone may interact with the electropositive aromatic edge of Trp60D (3.7 Å), but such an interaction is necessarily weak. The peptide nitrogen of the methionine sulfone is hydrogen-bonded to Gly216 O (2.9 Å) but the carbonyl is rather distant from Gly216N (3.5 Å). The N-terminal benzyl group occupies the S3 subsite making van der Waals contacts with Trp215 in an edge to face fashion[19] similar to the D-Phe group of PPACK, although the positions of the aromatic rings of the two inhibitors are not coplanar. The benzyl group also makes hydrophobic contacts with Leu99 and Ile174. The sulfone group linking the terminal benzyl group with the remainder of the inhibitor approaches the Cγ of Glu217 (3.4 Å) and Gly216 O (3.4 Å).

The cleavage of the inhibitor results in a C-terminal arginyl derivative with a free α-keto acid (Fig. 4). This group interacts with thrombin in an unusual manner compared to the APP–trypsin complex. As usual, the side chain oxygen of the active site Ser195 is close (1.6 Å) to the keto carbon of the inhibitor forming a hemiketal. The keto oxygen, however, is 'flipped around' (i.e. rotated approximately 180°) the Cα and keto carbon bond as compared to the usual carbonyl binding in the active site of serine proteases (Fig. 4). It is therefore not located in the oxyanion hole but hydrogen bonds to His57 Nε2 (2.4 Å), which hence must be protonated at this relatively high pH (7.3). The oxyanion hole is instead occupied by the negatively charged terminal carboxyl group of the inhibitor (Fig. 5). One of its oxygens makes better hydrogen bond contacts with the main chain hydrogen bond donors Gly193 N and Ser195 N (2.6 and 2.7 Å, respectively) than is usually observed with carbonyl groups in the thrombin oxyanion hole, whereas the other is within hydrogen bond distance to three water molecules. The carbonyl carbon to oxygen vector of the inhibitor is 24° out of the plane defined by the Cα, C and carboxylate carbon, and the torsion angle between carbonyl and carboxylate is 73°. The nitrogen atoms of Gly192, Asp194 and Ser195 deviate from those in the hirugen structure by only 0.1–0.3 Å in the CVS-1347–thrombin structure compared to 0.5–1.0 Å in PPACK–thrombin. The Glu192 conformation is also different from that observed in the PPACK–thrombin structure and points away from the active site as in hirugen–thrombin, apparently due to the presence of the bulky electronegative methionine sulfone and the negatively charged carboxylate terminal of the inhibitor. A similar orientation occurs when the P3 site is occupied with an aspartate.[9]

Discussion

There have been numerous reports describing the incorporation of the α-keto amide transition-state functionality into inhibitors of serine proteases.[20,22] The only reported example of a serine protease inhibitor containing a P1 substituted α-keto arginine described to date is cyclotheonamide A, a natural inhibitor originally isolated from the marine sponge *Theonella*[23] and recently synthesized.[13,24] Both cyclotheonamide A,[25] as well as CVS-1347, share a similar mechanism of thrombin inhibition, which involves the formation of a single EI complex. In addition, both inhibitors can be characterized as kinetically slow-binding, which has also been observed for other α-keto amides containing a different P1 side chain.[22] The relative K_i values for cyclotheonamide A (K_i = 1.0 nM)[25] compared to CVS-1347 (K_i = 0.129 nM) differ, most likely due to the more favorable side chain interactions between CVS-1347 and enzyme at specificity subsites within the active site beyond the S1 site.

Binding of an active site inhibitor to hirugen–thrombin to form a ternary complex has been shown not to alter the overall conformation of the enzyme. This is also true for the hydrolyzed form of CVS-1347. The inhibitor belongs to a class of active site inhibitors with a Pro–Arg dipeptide core that has been designed to improve selectivity and binding potency for thrombin. These inhibitors bind as substrate or transition state analogs in an anti-parallel β-strand fashion hydrogen–bonded with residues Ser214 and Gly216. The Pro–Arg group binds in the S1 and S2 subsites of the enzyme active site, respectively. The position of the methionine sulfone residue of the inhibitor was only weakly defined in the structure due to large thermal motion and lack of contacts with the enzyme. The residue therefore probably contributes little to the bound state of the inhibitor. However, the high potency of CVS-1347 compared to inhibitors with other P3 residues suggests that Met(O_2) has a beneficial effect on the solution conformation of this inhibitor. In any approach to improve inhibitor binding, the choice of this side chain should be re-evaluated. Its position is delicate since consideration has to be taken of both the positively charged arginine P1 of the inhibitor and the negatively charged Glu192 of thrombin. Substitutions at P3 that increase attraction with the negative hydrogen bond acceptor Glu192 necessarily would decrease that between the P3 position and the positively charged P1 hydrogen bond donor. The attraction between P1 and P3 may be important since it could stabilize conformations of the

inhibitor in solution that are similar to that of the bound state (i.e. note proximity of P3 to P1 in Fig. 4), thus reducing the negative entropy of binding. This could possibly be resolved by the introduction of a basic residue crosslinked to the P1 residue. Moreover, Glu192 is not conserved among serine proteases and offers an opportunity of specificity, which might be more important than maximum binding strength from a pharmacological point of view. Slight reduction of thrombin affinity might be compensated by a marked reduction of affinity for non-target serine proteases. Care must also be taken to distinguish between the intact CVS-1347 peptide and the hydrolyzed adduct described here, since the electrostatic properties differ considerably, with the latter possessing a free carboxylate group and a net charge of zero, whereas intact CVS-1347 has a net charge of plus one. For steric and electronic reasons the sulfone group of the P3 residue repels Glu192 from the active site compared to that of PPACK–thrombin.[9] The flexibility of Glu192 is in accordance with its general lack of hydrogen bond contacts and its high B-values.

The N-terminal benzyl group of the inhibitor makes hydrophobic and aromatic contacts with the hydrophobic S3 subsite of the active site, similar but not identical to D-Phe of PPACK. The linking sulfone part of the *N*-benzylsulfonyl group appears to orient the terminal aromatic ring properly for interaction with Trp215 and might therefore contribute to inhibitor binding indirectly, even though its direct contacts with the enzyme are limited. In this respect it appears to play the same role as the D-configuration of the N-terminal phenylalanine residue in PPACK.

The bound structure of the C-terminus of the inhibitor is as surprising as its cleavage. Due to hydrolysis of the α-keto amide bond, an α-keto group is exposed near the catalytic triad with a covalent distance between the carbon atom and Ser195 Oγ. Since the keto oxygen is hydrogen bonded to His57 the latter must be protonated in the crystallographic structure. This and the fact that it must be deprotonated for nucleophilic attack as in the PPACK–thrombin structure is in agreement with the reported p*K* of 7.3,[26] which is also the pH of the crystallization mother liquor. Another thrombin inhibitor that has an intact α-keto amide group adjacent to the arginine P1 side chain is the macrocycle cyclotheonamide A. This keto group occupies the oxyanion hole of thrombin,[13] as would be expected from analogy with the PPACK structure. In the present structure, the carboxylate is located in the oxyanion hole instead of the keto oxygen and appears to fit better than a carbonyl group.

The binding of the hydrolyzed adduct of CVS-1347 contrasts with yet another structure of a serine protease inhibitor complex: the α-keto carboxylate APP binds to the active site of trypsin[18] with the keto group hydrogen bonded to the Gly193 and Ser195 nitrogen atoms of the oxyanion hole while the carboxylate is hydrogen-bonded to His57 of the catalytic triad. In the thrombin complex, the situation is reversed. This supports the supposed role of the oxyanion hole in the catalytic mechanism of the serine proteases since the oxyanion hole here shows a preference for a negatively charged group and hence could stabilize an oxyanion transition state. The deviation from planarity and the torsion angle relative to the carboxylate are 37° and 28°, respectively in the APP–trypsin complex but are 24° and 73° in the thrombin complex. The α-keto group of the latter thus appears to be in an energetically more favorable conformation. The two structures demonstrate that the protonated histidine and the oxyanion hole have similar chemical properties, or affinities, since that which applied for the one in the present structure, is true for the other in the APP–trypsin structure. Additionally, the position of the keto oxygen shows that histidine can act as a hydrogen bond donor towards an atom adjacent to the carbonyl carbon atom subjected to nucleophilic attack by Ser195. What occurs here might thus be analogous to a transition state where the serine hydrogen is donated to the substrate nitrogen via the histidine. In both cases, the serine acts as a nucleophile and the histidine as a proton donor to a pair of adjacent inhibitor/substrate atoms. This confirms the role that the histidine is generally thought to have as a proton donor towards the amide nitrogen of the substrate and the dual role as proton donor/acceptor further justifies its position in the catalytic machinery of the serine and cysteine proteases.

Experimental

Synthesis of CVS-1347 (Fig. 6)

Preparation of methioninesulfoneproline benzylester hydrochloride. To a solution of *t*-butoxycarbonylmethioninesulfone acid (14.0 g, 50.0 mmol) in dichloromethane (150 mL) at 0 °C was added *N*-hydroxybenzotriazole (HOBt) (10.1 g, 75 mmol) followed by dicyclohexylcarbodiimide (DCC) (11.33 g, 55.0 mmol). The mixture was stirred for 10 min, and then proline benzylester hydrochloride salt (50.0 mmol, 12.0 g) was added followed by *N*-methylmorpholine (NMM) (100 mmol, 10.9 mL). The resulting mixture was stirred in an ice bath and allowed to come to room temperature over 12 h. The mixture was then filtered to remove dicyclohexylurea and ethyl acetate (300 mL) was added. The organic phase was then added to a separatory funnel and washed with saturated aqueous sodium bicarbonate, brine and then 1 N aqueous HCl. The organic phase was dried over magnesium sulfate, filtered and reduced on a rotary evaporator *in vacuo* to provide 23.5 g of a white solid (100%); $R_f = 0.34$ (silica gel; chloroform:methanol, 95:5).

To a solution of *t*-butoxycarbonylmethioninesulfoneproline benzylester (23.5 g, 50 mmol) in dry dioxane (300 mL) was added 100 mL of a 4 M HCl dioxane solution. The mixture was then stirred at room temperature for 1 h until the starting material disappeared as shown by thin layer chromatography analysis (chloroform:methanol, 90:10). Diethyl ether was added to the

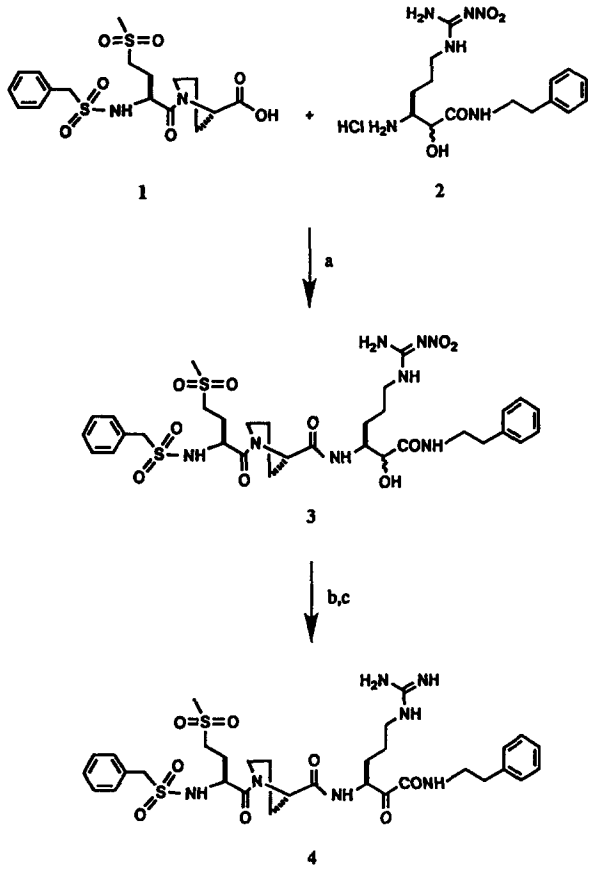

Figure 6. Synthesis scheme for the preparation of CVS-1347 (**4**); (a) DMF, BOP, NMM; 70%; (b) PhMe, DMSO, EDC, DCA; 51%; (c) HF, anisole; 30%.

mixture to precipitate the white hydrochloride salt. The mixture was filtered on a Buchner funnel and then dried under high vacuum to provide 20.16 g (100%) of a white solid.

Preparation of α-toluenesulfonylmethioninesulfoneproline (1). To a solution of methioninesulfoneproline benzylester hydrochloride (20.0 mmol, 8.08 g) in dry acetonitrile (CH_3CN) (100 mL) cooled to 0 °C was added α-toluenesulfonylchloride (20.0 mmol, 3.8 g) all at once, followed by pyridine (50.0 mmol, 4.2 mL). The mixture was then stirred in an ice bath for 12 h eventually warming to room temperature. Work-up consisted of reducing the volume *in vacuo* and diluting with ethyl acetate (300 mL). The organic phase was then washed with saturated aqueous sodium bicarbonate, brine and 1 M aqueous HCl (100 mL). The organic phase was dried over magnesium sulfate, filtered and evaporated *in vacuo* to provide 8.8 g (100%) of a foamy golden solid; R_f = 0.31 (silica gel; chloroform:methanol, 95:5).

The solid was filtered through a plug of silica gel (50 g) using ethylacetate (to eliminate possible sulfur related impurities) and concentrated to a white foam which was dissolved in methanol (300 mL), purged with nitrogen, and added to 1.0 g of 10% Pd/C. The mixture was then stirred vigorously under H_2 at 1 atm and room temperature for 12 h. The mixture was then filtered and the organic phase reduced *in vacuo* to provide 8.0 g (100%) of **1** (Fig. 6) as a white foam; R_f = 0.21 (silica gel; dichloromethane:methanol, (90:10); mp 68–71 °C and mass spectrum (FAB) shows the expected molecular ion of M + H 434. NMR (400 MHz, $CDCl_3$, reference chemical shift 7.27 ppm, 25 °C, 23 mM **1**) phenyl-CH_2-SO_2-: δ 7.36–7.43 (5H, *m*, phenyl), δ 4.31 (1H, *d*, *J* = 13.9 Hz, CH_2), δ 4.39 (1H, *d*, *J* = 13.9 Hz, CH_2); Met(O_2) [-HN-CHα-($CHβ_2$-$CHγ_2$-SO_2-$CHε_3$)-CO-]: δ 6.58 (1H, *d*, *J* = 8.9 Hz, HN), δ 3.91 (1H, *ddd*, *J* = 8.9, 8.1, 4.2 Hz, Hα), δ 1.94 (1H, *m*, Hβ), δ 2.09 (1H, *m*, Hβ), δ 3.11 (2H, *m*, Hγ), δ 2.96 (3H, *s*, Hε); Pro [N-CHα-($CHβ_2$-$CHγ_2$-$CHδ_2$-)-CO_2H]: δ 4.39 (1H, *dd*, *J* = 5.6, 8.4 Hz, Hα), δ 1.91 (1H, *m*, Hβ), δ 2.24 (1H, *m*, Hβ), δ 2.01 (2H, *m*, Hγ), δ 3.05 (1H, *m*, Hδ), δ 3.37 (1H, *m*, Hδ).

Preparation of tripeptide-hydroxyamide (3). A 1.5 g (3.31 mmol) portion of the N-α-Boc-arginine(Ng-nitro)hydroxyamide (WO 94/08941) was taken up in 40 mL of dichloromethane and added to 40 mL of trifluoroacetic acid at 0 °C, and stirred for 1 h. This salt was precipitated with diethyl ether and dried *in vacuo* to provide **2** (Fig. 6).

This residue was dissolved in 17 mL dimethylformamide (DMF) and 1.4 g (3.31 mmol) of α-toluenesulfonylmethioninesulfoneproline (**1**) was added followed by 1.6 g (3.65 mmol) of benzotriazol-1-yloxy-tris-(dimethylamino)-phosphonium hexafluorophosphate (BOP) and 1.00 mL (8.95 mmol) of NMM and the solution was allowed to stir overnight. This solution was dissolved in 200 mL ethyl acetate and washed with water, 1 N aqueous HCl, water, saturated sodium bicarbonate and brine (150 mL each). The solution was dried over magnesium sulfate and concentrated *in vacuo* to give, after purification by column chromatography (silica gel; dichloromethane:methanol 90:10), 1.8 g (70%) of the above compound as an off-white foam; R_f = 0.29 (silica gel; dichloromethane: methanol, 90:10).

Preparation of tripeptide-ketoamide CVS-1347 (4). A 1.8 g (2.34 mmol) portion of **3** (Fig. 6) was taken up in 47 mL of 1:1 toluene (PhMe):dimethylsulfoxide (DMSO) with ethyl-3-(3-dimethylamino)-propyl carbodiimide hydrochloride (EDC) (4.5 g, 23.47 mmol). To this solution was added 0.77 mL (2.42 mmol) of dichloroacetic acid (DCA). This solution was stirred for 70 min, diluted with 200 mL water and extracted twice with ethyl acetate (350 mL). The organics were combined, washed with saturated sodium bicarbonate and brine, dried over magnesium sulfate and concentrated *in vacuo*. This solution was purified on a silica column (4:1:4, hexanes:methanol:dichloromethane) to give 918 mg (51%) of the ketone as a white foam; R_f = 0.26 (silica gel; dichloromethane: methanol, 90:10).

This product was subjected to hydrogen fluoride (using a standard HF apparatus and procedure for peptide deprotections using anisole) and purified by HPLC (50 mm × 30 cm Vydak C-18 column, gradient of 10–35%

B where B = CH_3CN and A = H_2O with 0.1% TFA, at a flow rate of 115 mL min^{-1}) to give 300 mg (30%) of the final compound as the TFA salt after lyophilization, which had an actual mass spectral peak (FAB, M + H 614.2) that correlated well with the expected value of M + H 614.3. The product was analyzed by 1D and 2D-COSY NMR (400 MHz, D_2O, reference chemical shift 4.78 ppm, 50 mM pH 2 phosphate buffer, 25 °C, 11.8 mM **4**). Phenyl-CH_2-SO_2-: δ 7.25–7.41 (5H, *m*, phenyl), δ 4.47 (1H, *d*, *J* = 14.3 Hz, CH_2), δ 4.58 (1H, *d*, *J* = 14.3 Hz, CH_2); Met(O_2) [-HN-CHα-($CH\beta_2$-$CH\gamma_2$-SO_2-$CH\varepsilon_3$)-CO-]: δ 3.93 (1H, *dd*, *J* = 4.84, 8.82 Hz, Hα), δ 1.93 (1H, *m*, Hβ), δ 2.10 (1H, *m*, Hβ), δ 3.24 (2H, *m*, Hγ), δ 3.08 (3H, *s*, Hε); Pro [-N-CHα-($CH\beta_2$-$CH\gamma_2$-$CH\delta_2$-)-CO-]: δ 4.26 (1H, *dd*, *J* = 5.77, 8.35 Hz, Hα), δ 1.78 (1H, *m*, Hβ), δ 2.16 (1H, *m*, Hβ), δ 1.87 (2H, *m*, Hγ), δ 3.03 (1H, *m*, Hδ), δ 3.34 (1H, *m*, Hδ); Arg(CO) [-HN-CHα-($CH\beta_2$-$CH\gamma_2$-$CH\delta_2$-guan)-CO-CO_2H]: δ 4.02 (1H, *d*, *J* = 9.76 Hz, Hα), δ 1.38 (1H, *m*, Hβ), δ 1.59 (1H, *m*, Hβ), δ 1.49 (1H, *m*, Hγ), δ 1.59 (1H, *m*, Hγ), δ 3.11 (2H, *m*, Hδ); -$CH\alpha_2$-$CH\beta_2$-phenyl: d 7.43–7.51 (5H, *m*, phenyl), δ 3.42 (1H, *dt*, *J* = 13.6, 6.9 Hz, Hα), δ 3.50 (1H, *dt*, *J* = 13.6, 6.9 Hz, Hα), δ 2.84 (2H, *m*, Hβ).

Other materials

The concentration of CVS-1347 was based on the level of proline using quantitative amino acid composition on replicate samples following acid-hydrolysis and analysis using a Beckman Model 6300 analyzer. Purified, human α-thrombin (3,806 NIH units mg^{-1}) used in bioassays was purchased from Enzyme Research Laboratories, Inc. (South Bend, IN) and quantitated by the absorbance of a solution at 280 nm using $e^{1\%} = 18.3$ and an M_r of 36,500.[27] The enzymatic activity of thrombin was measured, using the chromogenic substrate Pefachrome tPA (CH_3SO_2-D-hexahydro-tyrosine-glycyl-arginine-*p*-nitroanaline·AcOH) which was obtained from Pentapharm, Ltd (Basel, Switzerland). The substrate was reconstituted in deionized water prior to use. The α-thrombin and hirugen used for crystallization were generously supplied by Dr John Fenton, II (New York State Department of Health) and Dr John Managanore (Biogen), respectively.

Kinetics of thrombin inhibition

The amidolytic activity of α-thrombin was measured in triplicate at ambient temperature (22–25 °C) in a 96-well microtitre plate (Corning), using a ThermoMax® kinetic microplate reader (Molecular Devices, Sunnyvale, CA) which recorded the change in absorbance at 405 nm over 60 min at 15 sec intervals. The reactions were initiated by the addition of 50 μL of α-thrombin to wells, containing 100 μL of the substrate, (Pefachrome tPA), and 100 μL of CVS-1347, or in the case of a control, 100 μL of HBS (10 mM HEPES, 150 mM NaCl, and bovine serum albumin, 0.1%, w/v, pH 7.5). The final concentrations of reactants in a total of 250 μL were: 200 pM thrombin, 0–12 nM CVS-1347, and 750 μM Pefachrome tPA (17 × K_m). All reactions were performed under steady-state conditions, where less than 6% of the substrate was consumed. The absorbance data, depicting the progress curves were exported, and fit directly, using Inplot™ (GraphPad Software, Inc., San Diego, CA), by nonlinear regression to the integrated first-order rate equation 1.[16,17]

$$P = V_s t + (V_o - V_s)\,(1 - e^{-k_{obs}t})\,/k_{obs} \qquad (1)$$

This equation describes the slow establishment of equilibrium between enzyme and competitive inhibitor where P is the measured absorbance defined as a function of the initial (V_o) and final (V_s) steady-state velocities. The apparent first-order rate constant (k_{obs}), describes the equilibrium from the initial to the final steady-states. The rate constants describing the inhibition of thrombin by CVS-1347 were calculated using equation 2, which describes the slow formation of a single EI complex where there is a linear relationship between the inhibitor concentration [I] (0.2–12 nM) and k_{obs}.[17]

$$k_{obs} = k_1\,[I]/(1 + [S]/K_m) + k_{-1} \qquad (2)$$

The values for the second-order association rate constant (k_1) for the formation of the enzyme–inhibitor complex and the first-order dissociation rate constant (k_{-1}) were determined at a fixed substrate ([S]) concentration as described above using a predetermined K_m of 45 μM. The equilibrium dissociation rate constant K_i was calculated from the ratio k_{-1}/k_1.

Crystallization

A 1 mL sample of frozen thrombin (1.06 mg mL^{-1} in 0.75 M NaCl) was thawed on ice after addition of a 10-fold molar excess of solid hirugen and then 1 mL of 0.1 M sodium phosphate (pH 7.3) and 1 mM NaN_3 was added to the resulting solution. A 10-fold molar excess of CVS-1347 dissolved in 50 μL of methanol was mixed with the enzyme solution and the sample concentrated to 0.25 mL through centrifugation with Centricon-10 concentrators. The inhibited enzyme was incubated as hanging drops in a 1:1 mixture with the equilibrating solution, which was 25% PEG 8000, 0.1 M phosphate buffer (pH 7.3) and 1 mM NaN_3. Seeds of thrombin–hirugen crystals were added after 24 h of equilibration and the newly formed crystals were enlarged through macroseeding as was done in the original crystallization of PPACK–thrombin.[28]

Crystallography

Diffraction data of one crystal specimen were collected using a Rigaku R-AXIS II imaging plate detector and a Rigaku RU200 fine focus rotating anode operating at 50 kV and 100 mA. The monoclinic crystals belong to space group C2 with one ternary complex per asymmetric unit and cell parameters a = 71.08, b = 72.05 and c = 72.98 Å and β = 100.8° that are isomorphous with those of hirugen–thrombin crystals.[8] Intensity data

collection statistics are given in Table 1. The structure of the protein–ligand complex was refined[29,30] starting with a model consisting of the light and heavy chains of the hirugen–thrombin structure with the program PROLSQ in the range (8.00–1.76) Å with a cutoff of 2.0σ on $|F|^2$. During the course of the restrained refinement, hirugen, the hydrolyzed CVS-1347 inhibitor and water molecules were successively included to fit (2|Fo| – |Fc|) and (|Fo| – |Fc|) maps calculated by PROTEIN[31] and displayed on an Evans and Sutherland PS390 stereographics station with the program O.[32] The final structure with 161 water molecules has an R-value of 0.162 and the final refinement statistics are presented in Table 2.

Table 1. Intensity data collection summary

Shell (Å)	Average Intensity	Average I/σ(I)	# of Reflections Obsr.	Theoretical	Completeness (%) Shell	Cumulative	Rmerge (%) Shell	Cumulative
15.00	941	21.5	51	73	69.9	69.9	3.2	3.2
10.00	1592	20.9	130	152	85.5	80.4	2.9	3.0
7.50	1072	20.0	272	299	91.0	86.5	3.6	3.3
5.00	866	18.5	1083	1172	92.4	90.6	4.0	3.8
3.50	1133	18.5	2903	3117	93.1	92.2	4.1	4.0
3.00	420	16.1	2488	2730	91.1	91.8	4.5	4.1
2.70	209	13.1	2441	2763	88.3	90.9	5.4	4.2
2.40	117	10.3	3654	4282	85.3	89.3	6.3	4.3
2.00	58	6.3	7999	10439	76.6	84.0	8.9	4.6
1.76	18	2.6	5417	11461	47.3	72.5	14.9	4.7
Totals:			26438	36488				

Table 2. Refinement results

	Target sigma	rmsΔ
Distances		
Bond distance (Å)	0.02	0.024
Angle distance (Å)	0.03	0.052
Planar 1–4 distance (Å)	0.06	0.066
Miscellaneous		
Plane groups (Å)	0.020	0.018
Chiral centers (Å^3)	0.150	0.208
Non-bonded distances		
Single torsion (Å)	0.50	0.24
Multiple torsion (Å)	0.50	0.28
Possible X–Y H-bond (Å)	0.50	0.26
Torsion angles		
Planar (°)	3.0	3
Staggered (°)	15.0	21
Orthonormal (°)	20.0	32
Thermal restraints		
Main-chain bond (Å^2)	2.0	2.0
Main-chain angle (Å^2)	3.0	2.8
Side-chain bond (Å^2)	3.0	3.5
Side-chain angle (Å^2)	4.0	4.7
Diffraction pattern		
$\sigma\|Fo\| = A + B[\sin\theta/\lambda - 1/6]$		
A	23.0	51.9
B	–125.0	–374.3

Table 2. Refinement results (continued)

Resolution	Number of reflections	<Fo – Fc>	Shell R_{Cryst}	Sphere R_{Cryst}
3.28	4949	75.9	0.148	0.148
2.63	4538	43.8	0.164	0.153
2.31	4075	31.3	0.176	0.157
2.10	3700	25.3	0.178	0.159
1.95	2813	20.7	0.188	0.160
1.84	1542	17.9	0.209	0.162
1.75	650	15.6	0.217	0.162
All	22267	40.1		0.162

Acknowledgements

This work was supported by NIH Grant HL 43229. We also thank Dr K. Padmanabhan, Dr K. P. Padmanabhan and Dr I. I. Mathews for their help at various stages of this work and Dr Eugene Zaluzec, Department of Biochemistry (MSU) for MALDI–MS measurement.

References

1. Scheraga, H. A.; Laskowski, M. *Adv. Protein Chem.* **1957**, *12*, 1.

2. Butkowski, R. J.; Elion, J.; Downing, M. R.; Mann, K. G. *J. Biol. Chem.* **1977**, *252*, 4942.

3. Degen, S. J. F.; Davie, E. W. *Biochemistry* **1987**, *26*, 6165.

4. Bode, W.; Mayr, I.; Baumann, U.; Huber, R.; Stone, S. R.; Hofsteenge, J. *EMBO J.* **1989**, *8*, 3467.

5. Markwardt, F. *Methods Enzymol.* **1970**, *19*, 924.

6. Dodt, J.; Machleidt, W.; Seemüller, U.; Maschler, R.; Fritz, H. *Biol. Chem. Hoppe-Seyler* **1986**, *367*, 803.

7. Rydel, T. J.; Ravichandran, K. G.; Tulinsky, A.; Bode, W.; Huber, R.; Roitsch, C.; Fenton, J. W. *Science* **1990**, *249*, 277.

8. Skrzypczak-Jankun, E.; Carperos, V. E.; Ravichandran, K. G.; Tulinsky, A.; Westbrook, M.; Maraganore, J. M. *J. Mol. Biol.* **1991**, *221*, 1379.

9. Vijayalakshmi, J.; Padmanabhan, K. P.; Mann, K. G.; Tulinsky, A. *Protein Sci.* **1994**, *3*, 2254.

10. Leforits, J.; Topol, E. J. *Circulation* **1994**, *90*, 1522.

11. Brundish, D. E. *Current Opinion in Therapeutic Patents* **1992**, 2, 1457.

12. Tapparelli, C.; Metternich, R.; Ehrhardt, C.; Cook, N. S. *Trends Pharmacol. Sci.* **1993**, *14*, 366.

13. Maryanoff, B. E.; Qiu, X.; Padmanabhan, K. P.; Tulinsky, A.; Almond, H. R.; Andrade-Gordon, P.; Greco, M. N.; Kauffman, J. K.; Nicolaou, K. C.; Liu, A.; Brungs, P. H.; Fusetani, N. N. *Proc. Natl Acad. Sci. U.S.A.* **1993**, *90*, 8048.

14. Lee, A. Y.; Haghihara, M.; Karmacharya, R.; Albers, M. W.; Schreiber, S. L.; Clardy, J. *J. Am. Chem. Soc.* **1994**, *1*, 10.

15. Lee, A. Y.; Clardy, J. *J. Chem. Biol.* **1994**, *1*, 10.

16. Cha, S. *Biochem. Pharmacol.* **1975**, *24*, 2177.

17. Williams, J. W.; Morrison, J. F. *Methods Enzymol.* **1979**, *63*, 437.

18. Walter, J.; Bode, W. *Physiol. Chem.* Hoppe-Seyler **1983**, *364*, 949.

19. Burley, S. K.; Petsko, G. A. *Science* **1985**, *229*, 23.

20. Ocain, T. D.; Rich, D. H. J. *J. Med. Chem.* **1992**, *35*, 451.

21. Hu, L. Y.; Ables, R. H. *Arch. Biochem. Biophys.* **1990**, *281*, 271.

22. Paris, M. F.; Ables, R. H. *Biochemistry* **1992**, *31*, 9429.

23. Fusetani, N.; Matsunaga, S.; Matsumoto, H.; Takebayashi, Y. *J. Am. Chem. Soc.* **1990**, *112*, 7053.

24. Haghihara, M.; Schreiber, S. L. *J. Am. Chem. Soc.* **1992**, 114, 6570.

25. Lewis, S. D.; Ng, A. S.; Baldwin, J. J.; Fuestani, N.; Naylor, A. M.; Shafer, J. A. *Thromb. Res.* **1993**, *70*, 173.

26. Stone, S. R.; Maraganore, J. M. In: *Thrombin Structure and Function*, pp. 219–256, Berliner, L. J., Ed.; Plenum Press; New York, 1992.

27. Fenton, II J. W.; Fasio, M. J.; Stackrow, A. B.; Aronson, D. L.; Young, A. M.; Finlayson, J. S. *J. Biol. Chem.* **1977**, *252*, 3587.

28. Skrzypczak-Jankun, E.; Rydel, T. J.; Tulinsky, A.; Fenton, II J. W.; Mann, K. G. *J. Mol. Biol.* **1989**, *206*, 755.

29. Hendrickson, W. A. *Methods Enzymol.* **1985**, *115*, 252.

30. Finzel, B. C. *J. Appl. Crystallogr.* **1987**, *20*, 53.

31. Steigemann, W. Ph.D. thesis, Technische Universität, Munich, 1974.

32. Jones, T. A.; Zou, J.-Y.; Cowan, S. W.; Kjeldgaard, M. *Acta Crystallogr. A.* **1991**, *47*, 110.

(*Received in U.S.A.* 5 *January* 1995)